The Warm Receiver Section and the Digital Backend of the PHAROS2 Phased Array Feed

A. Navarrini[1], A. Scalambra[2], A. Melis[1], S. Rusticelli[2], R. Concu[1], P. Ortu[1], G. Naldi[2], G. Pupillo[2], A. Maccaferri[2], A. Cattani[2], A. Ladu[1], L. Schirru[1], F. Perini[2], M. Morsiani[2], J. Monari[2], J. Roda[2], P. Marongiu[1], A. Saba[1,5], M. Poloni[2], M. Schiaffino[2], A. Mattana[2], G. Bianchi[2], G. Comoretto[3], R. Nesti[3], E. Urru[1],T. Pisanu[1], F. Schillirò[4], K. Zarb Adami[6,7], A. Magro[6], R. Chiello[7]

[1]INAF (National Institute for Astrophysics)-Astronomical Observatory of Cagliari, Selargius, Italy
[2]INAF (National Institute for Astrophysics)-Institute of Radio Astronomy, Bologna, Italy
[3]INAF (National Institute for Astrophysics)-Arcetri Astrophysical Observatory, Florence, Italy
[4]INAF (National Institute for Astrophysics)-Astrophysical Observatory of Catania, Catania, Italy,
[5]ASI (Italian Space Agency), Rome, Italy
[6]University of Malta, Malta
[7]University of Oxford, Department of Physics, United Kingdom

***Abstract*—We describe the development of a multi-channel "warm receiver section" (WS) and of a digital beamformer for the PHAROS2 Phased Array Feed (PAF), a PAF demonstrator for radio astronomy application across the 4-8 GHz radio frequency (RF) band. The PAF is based on an array of 10×11 dual-polarization Vivaldi antennas cryogenically cooled at 20 K along with low noise amplification modules (LNAs). The WS receiver can process the signals from a subset of 24 antenna elements of the array by downconverting them to an intermediate frequency (IF) range, 375-650 MHz, suitable for digitization by the digital beamformer. The latter is based on the iTPM (Italian Tile Processing Module), developed for the Square Kilometer Array (SKA) Low Frequency Aperture Array (LFAA). We modified the iTPM firmware to synthesize four independent beams across the 275 MHz instantaneous IF bandwidth in the iTPM FPGAs (Field Programmable Gate Arrays). The 24 signals are sent from the WS to the iTPM through analogue IFoF (IF over fiber) optical links. In this paper we present the design and performance of the WS and of the digital bemaformer for PHAROS2.**

Keywords—phased array feed, heterodyne, filter bank, fiber-optic link, radio astronomy, digital backend, beamformer.

I. Introduction

High-sensitivity large-scale surveys are an essential tool for new discoveries in radio astronomy. A PAF placed at the focal plane of an antenna can increase the Field-of-View (FoV) and the mapping efficiency by fully sampling the sky [1]-[2]-[3]. A PAF consists of closely packed antenna elements with about half wavelength element separation that, by spatially sampling the focal plane, can synthesize multiple independent beams and be set to Nyquist-sample the sky. Multiple beams are formed by electronically adding the signals from different groups of radiating elements of the array. An antenna element can contribute to form multiple beams. The properties of the beams can be optimized over a wide range of frequencies by electronically controlling each element phase and amplitude (complex weights) leading to high aperture efficiency and low spillover.

PHAROS (PHased Arrays for Reflector Observing Systems) [4]-[7] is a cryogenically cooled PAF demonstrator with analogue beamformer based on an array of dual-polarization 10×11 Vivaldi antennas designed for radio astronomy observation across the 4-8 GHz band. The array, shown in Fig. 1, is cooled to 20 K along with 24 low noise amplifiers (LNAs) mounted directly behind the array elements.

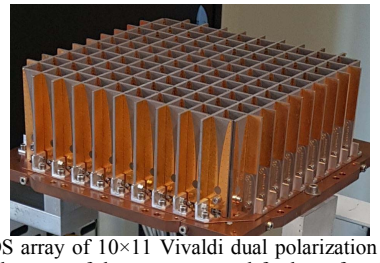

Fig. 1. PHAROS array of 10×11 Vivaldi dual polarization antennas. Only the 24 central elements of the array are used for beamforming, the rest are matched terminated.

PHAROS2 [8], the upgrade of PHAROS, is a cryogenically cooled PAF with digital beamformer for the 4-8 GHz band. The instrument is under development in the framework of the PAF SKA (Square Kilometer Array) [9] advanced instrumentation program. PHAROS2 is a technology demonstrator resulting from the international collaboration between the Italian National Institute for Astrophysics (INAF), Jodrell Bank Observatory at the University of Manchester (UK), ASTRON (the Netherlands), the University of Malta (Malta) and the University of Chalmers (Sweden).

A block diagram of the PHAROS2 PAF is illustrated in Fig. 2. The PAF features the following: *a)* a cryostat enclosing the PHAROS array of cryogenically cooled Vivaldi antennas, in which a sub-array of 24 antenna elements is cascaded with new generation LNAs with state-of-the-art performance (to reduce the system noise temperature); *b)* a 2.3-8.2 GHz room-temperature "Warm Section" (WS) multi-channel receiver; and *c)* an FPGA-based Italian Tile Processing Module (iTPM) digital backend [10] capable of digitizing and synthesizing four independent beams across a ≈275 MHz IF band from a sub-array of 24 antenna elements.

The development of the PHAROS2 cryogenic section is in charge to the University of Manchester and to the University of Chalmers, while the development of the warm receiver section (WS) and of the digital backend and beamformer, described in this paper, are in charge to INAF and to the University of Malta. The main specifications of the WS and of the digital backend are listed in Table I. The WS is required to handle up to 32 RF input signals, although only 24 will be used for PHAROS2. We note that the frequency range of the WS receiver, 2.3–8.2 GHz ($f_{max}/f_{min} \approx 3.6$), is greater than the one delivered by the PHAROS2 Vivaldi array cryogenic section (4–8 GHz). Therefore, the

978-1-7281-3049-1/19/$31.00 ©2019 IEEE

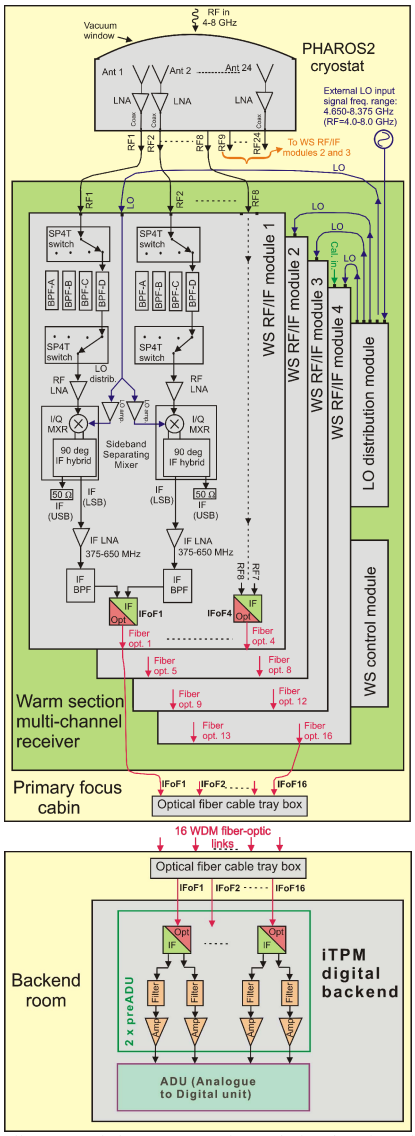

Fig. 2. Block diagram of the PAF receiver chain showing the PHAROS2 cryostat (top), the Warm Section multi-channel receiver (middle) and the iTPM digital backend (bottom). The schematic of the Warm Section multi-channel receiver, located in the primary focus receiver room, is enclosed by the green background rectangle.

WS and the associated digital backend can be used not only with PHAROS2, but also with other PAF antenna arrays that could be developed to cover 2.3–8.2 GHz.

The WS is a necessary piece of hardware for PAFs designed to operate beyond few GHz, as a direct sampling of the RF signal by analog to digital converters (ADCs) is currently possible up to several GHz. The existing high-performance ADCs have enough bits of resolution (typically 8–12) to operate in moderate radio frequency interference (RFI) environment, but limited bandwidth and maximum frequency, which makes them suitable solutions for PAFs radio astronomy application up to S-band (or lower frequency), but not yet for 4–8 GHz or beyond.

In section II we present the PHAROS Vivaldi antenna array. The design, construction, assembly and test of the PHAROS2 warm receiver section is discussed in section III, while the development of the digital backend and beamformer is discussed in section IV.

The PHAROS2 project aims at assembling, testing and installing the full PHAROS2 instrument (cryogenic section plus warm receiver section and digital backend) onto the 25-m diameter Pickmere radio astronomy antenna at the Jodrell Bank Observatory (operated by the University of Manchester), in order to conduct the technical and scientific commissioning that will refine the calibration and characterization of the PHAROS2 system. These will enable first-ever radio astronomy observations in C-band with a cryogenic PAF. Test results of the fully assembled PHAROS2 system on the radio astronomy antenna will be reported in a future paper.

TABLE I PHAROS2 WARM SECTION AND BACKEND SPECIFICATIONS

Warm receiver section	Number of RF channels	32 (four × eight-channel RF/IF modules). 24 used.
	RF band	2.3-8.2 GHz
	Frequency conversion scheme	Sideband Separating Mixer in LSB (USB terminated)
	LO band	2.950-8.575 GHz
	IF band	375-650 MHz
	Switched filter banks: Band Pass Filter freq. range and LO freq.	*BPF-A*: 2.300-8.200 GHz; LO tuning f_{LO}=2.95-8.575 GHz
		BPF-B: 4.775-5.050 GHz; fixed f_{LO}=5.425 GHz
		BPF-C: 5.780-6.055 GHz; fixed f_{LO}=6.430 GHz
		BPF-D: 6.445-6.720 GHz; fixed f_{LO}=7.095 GHz
	Signal transportation	Two IF output signals transported over a single optical fiber (IFoF) using WDM
	Number of WDM fiber-optics transmitters	16
	Control module	Optical fiber-Ethernet mediaconverter and microcontroller for BPF selection, LO power and PCB temperature monitoring
iTPM Digital backend	Number of WDM fiber-optics receivers	16
	ADCs	16 × dual-ADCs AD9680, 1 GS/s, ENOB=10.8
	FPGAs	2 × Xilinx Kintex Ultrascale XCU40 20 nm
	Number of synthesized beams and instantaneous coverage	Four beams implemented in the iTPM FPGAs for 24 antenna elements with 275 MHz bandwidth
	N. of frequency channels and resolution	512 channels, 0.81 MHz/ch. (32/27 overlapping factor)

II. PHAROS VIVALDI ARRAY

The PHAROS Vivaldi antenna array shown in Fig. 1 utilizes high-performance Taconic PCBs (TLY-5 substrate, with ε_r=2.20, tanδ=0.0008) with three-layer laminated board structure, based on two 1.14 mm thick substrates [5]. The antenna feed element is a stripline on the center conductor layer, sandwiched between the two board laminates. The complete PHAROS focal plane array antenna was built with 11 boards in both the *x* and the *y* directions, each integrating 10 Vivaldi elements with 21 mm spacing (Fig. 3). The spacing-to-wavelength ratio is 0.56 at the PHAROS/PHAROS2 maximum operating frequency of 8 GHz (λ_{min}≈37.5 mm). The overall size of the array on the *x*-*y* plane is ≈230×230 mm^2, i.e. ≈6λ_{min}×6λ_{min} (and equivalently

$\approx 3\lambda_{max} \times 3\lambda_{max}$ for $\lambda_{max} \approx 75$ mm, relative to the 4 GHz minimum frequency). A subset of 24 elements of the dual-polarization 10×11 Vivaldi antennas (220 elements) are connected to LNAs, the rest are matched terminated. The 24 active elements are located at the center of the array and excite the same polarization channel (antennas oriented on the *y*-plane). In PHAROS, a 13-element subarray of the 24 active elements (Fig. 4) is connected to a cryogenically cooled analogue beamformer. PHAROS was designed to integrate four identical analogue beamformers capable of forming four independent beams, each using a different combination of 13 elements of the 24 active ones. Some of the elements contribute to form more than one beam. Instead, in PHAROS2 all of the 24 same-polarization active antenna elements contribute to form each of the four independent beams synthesized by the digital backend [11].

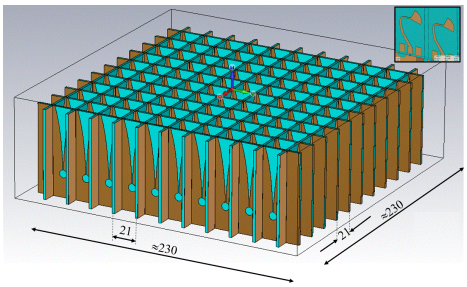

Fig. 3. 3D view of the PHAROS array of 10×11 dual-polarization Vivaldi antenna elements. Dimensions are in mm. The inset on the top right shows the detail of two of the antenna stripline feed elements.

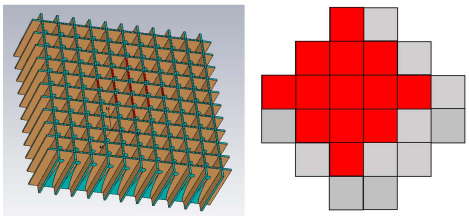

Fig. 4. Sub-array of 13 Vivaldi elements of the 24 active antennas connected to one analogue beamformer of the PHAROS PAF. Excited stripline antenna ports of Beam 1 (in red) and subset of the 24 active antennas (right panel).

III. Warm Section Multi-channel Receiver

The PHAROS2 warm section [12]-[13] is capable of analog processing up to 32 independent RF signals from the Vivaldi array, although only 24 are used.

A 3D view of the WS 32-channel receiver that we designed, assembled and tested, is given in Fig. 5. The WS includes four eight-channel WS RF/IF modules, one LO distribution module and one WS monitor and control module arranged in a standard 6U×19-inch rack. The receiver performs signal filtering by switched filter bank, signal conditioning, and single frequency down-conversion of a section of the 2.3-8.2 GHz RF band down to the 375-650 MHz IF band (275 MHz instantaneous bandwidth). The downconversion scheme utilizes sideband separating mixers in LSB (Lower Side Band). The IF signals are converted to optical signals by analogue WDM (Wavelength Division Multiplexing) "IFoF" (IF over fiber) fiber-optic transmitter (OTX) that transports two IFs over a single optical fiber. One of the four BPF filters, BPF-A, is specified to cover the broad 2.3-8.2 GHz RF frequency band, while the other three filters (BPF-B, -C and -D) have ≈275 MHz "narrowband" characteristics, with bands centered around astronomical lines.

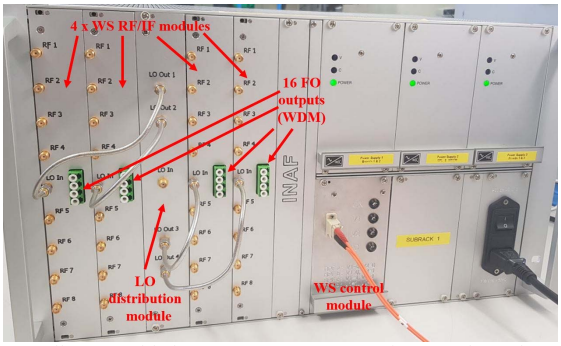

Fig. 5. Fully assembled PHAROS2 warm section 32-channel receiver showing the four WS RF/IF modules assembled with LO distribution module and WS control module arranged in a standard 19-inch × 6U rack.

We note that the frequency range of the WS receiver (2.3-8.2 GHz) is larger than the one delivered by the cryogenic section (4-8 GHz). Therefore, the room-temperature Front-End (and associated digital backend) can be used not only for application with the PHAROS2 cryogenic array, but also with other PAF antenna array that could be developed to cover the band 2.3-8.2 GHz ($f_{max}/f_{min}=3.4$) or part of it.

A. Eight-channel Warm Section RF/IF module

Each of the four WS RF/IF modules (Fig. 6) includes a PCB circuit and four WDM fiber-optic transmitters ("OTXs") on opposite sides of a mechanical support. The RF/IF module has eight SMA RF input connectors, one SMA LO input connector (centered on the front panel) and one quad LC/APC output connector to extract the four WDM IFoF optical fiber outputs provided by the four OTXs. The module employs a single four-layer PCB based on Rogers RG4003C substrate with thickness 0.508 mm and commercial surface-mounted components. The PCB adopts the standard double-height Eurocard size (6U, equivalent to ≈233.35 mm) that can be plugged into a standard chassis,

Fig. 6. Photos of the WS RF/IF module. Top left: mechanical housing (left) and fabricated PCB (right) before assembly. Microwave sbsorbers are glued in the pockets of the PCB mechanical housing. Top right: PCB board (first prototype version) and mechanical housing during assembly with optical transmitters. Bottom: Four WS RF/IF modules fully assembled, with OTXs.

978-1-7281-3049-1/19/$31.00 ©2019 IEEE

which in turn can be mounted in a 19-inch rack. The IF output signals are extracted from MCX connectors mounted orthogonal to the board. The board IFs outputs are connected to the WDM fiber-optics transmitter inputs through coaxial cables (Fig. 6, bottom panel).

The first element of the signal chain is a four-way switch filter-bank that allows selection of one of the four RF band pass filters through two SP4T switches. The filter bank is cascaded with an RF amplification stage followed by a sideband separating (2SB) mixer operated in single down conversion LSB mode. The 2SB mixer consists of a commercial I/Q mixer cascaded with a 90° IF hybrid that delivers two IF output signals to two independent ports. The USB output of the IF hybrid is terminated into a 50 Ω load, while its LSB output is band pass filtered and amplified. The IFs signal are routed to the on-board MCX connectors.

The PCB has one SMA connector for the LO input signal, centrally located on the RF side of the board. The LO signal is amplified, band pass filtered (by a cascade of low pass and high pass filters) and distributed internally to the PCB with one eight-way splitter based on a cascade of Wilkinson power dividers.

The PCBs and the mechanical housings were fabricated, respectively by Italian companies and INAF.

B. Warm section Local Oscillator distribution module

The four WS RF/IF modules receive a copy of the same LO signal from the LO distribution module (Fig. 5 and Fig. 7) so that the mixers (eight per board) are pumped under identical conditions. The 2.950-8.575 GHz four-way LO splitter utilizes Wilkinson power dividers and incorporates a directional coupler (coupling value ≈ -20 dB) that directs part of the signal to a detector. The detector allows converting the LO power to a decibel-scaled DC output used for monitoring purpose.

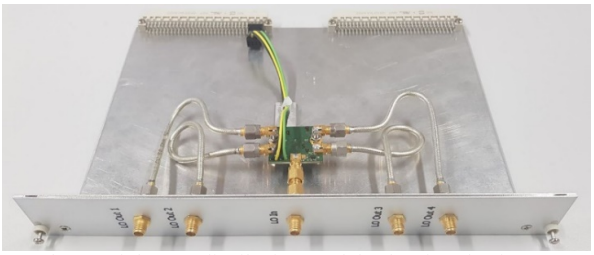

Fig. 7. Photos of the LO distribution module showing the four-way PCB LO splitter connected to the front panel SMAs through coaxial cables.

C. Warm Section monitor and control module

The WS monitor and control module (Fig. 8) is based on commercial optical fiber to Ethernet mediaconverter (Digitus DN-82010) and microcontroller (Arduino Leonardo ETH) incorporated into a 3U rack-mountable box biased with +5 V. The module utilizes transmitting/receiving mode with TX/RX multimode fiber and has two TTL outputs. It allows selection of one among four possible bandpass filters of the WS RF/IF modules and returns voltage values inversely proportional to the LO power of the LO distribution module. Furthermore, the module reads the physical temperature provided by the four sensors placed on the PCBs (one per board). The front-panel includes LEDs to visulaize the selected filter, the presence of LO power and of bias voltage.

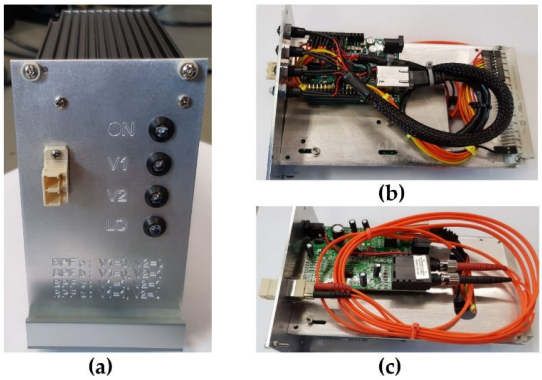

Fig. 8. Warm Section control module and its parts. (a) Front panel with TX/RX multimode fiber connector pair and LEDs. (b) Microcontroller by Arduino Leonardo ETH. (c) Optical fiber to Ethernet media-converter (Digitus DN-82010).

D. IF over fiber analogue links

The IFoF (IF over fiber) optical links were developed for SKA LFAA (Low Frequency Aperture Array, https://www.skatelescope.org/lfaa/) by an INAF-led collaboration with industrial partners and adopted for PHAROS2. The WDM IFoF technology utilizes dual distributed feedback (DFB) laser sources on the OTXs and dual photodiode detectors on the ORXs providing IF isolation between channels greater than 45 dB up to the maximum IF frequency (650 MHz). The signals are de-multiplexed at the optical receiver side. The optical (infrared) wavelengths at λ = 1270 nm and λ = 1330 nm were chosen to minimize the signal dispersion of the single-mode optical fibers (9/125 µm, G652D) across the IF band. The OTX optical lasers are class 3A, delivering an optical power at each of the two WDM wavelengths of less than 5 mW.

The ORXs are part of the iTPM digital backend (see section IV for further details). Each of the optical receivers utilizes two independent IF receiver chains that adapt the signals for digital conversion by the following iTPM Analog Digital Unit (ADU). Each of the ORX chains performs amplification and level adjustment through the digital step attenuators (DSAs) with 31 dB range and 1 dB step. The ORX control adopts the SPI bus from the ADU board. The maximum gain of the IFoF link is ≈60 dB when the DSA is set to its minimum attenuation of 0 dB (the link gain is of order ≈35 dB when setting the DSA to 25 dB).

E. Characterization of the warm receiver section

Two identical 32-channel receivers were fully assembled, although only one was required to equip the PHAROS2 PAF. The eight-channel WS RF/IF modules were characterized by INAF (Fig. 9). The modules perform according to technical specifications, and have similar performances. Fig. 10 shows an example of the measured receiver gains for the eight channels when the LO is set at a fixed frequency of 5 GHz and the RF is swept from 4 to 6 GHz (filter BPF-A selected). Vertical lines (in red) limit the nominal LSB (4350-4625 MHz) and USB (5375-5650 MHz) downconverted to the 375-650 MHz IF band. The receiver signal gain is in the range G_{LSB}=15-18 dB across the LSB (signal band) and below G_{USB}=-6 dB across the USB (image band). The image sideband rejection, i.e. the ratio between the conversion power gains IR=G_{LSB}/G_{USB} at the available IF port, is greater than 23 dBc across the nominal band.

978-1-7281-3049-1/19/$31.00 ©2019 IEEE

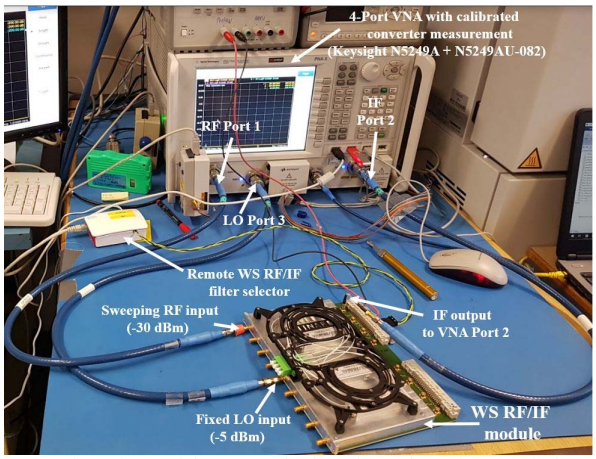

Fig. 9. Testing of one of the WS RF/IF boards (without the IFoF links). The RF port of the VNA is connected to ch. 1 of the board. The IF signal is extracted from the corresponding MCX connector.

We repeated the tests at 12 different LO frequencies, from 3 GHz to 8.5 GHz by 0.5 GHz steps, and measured the LSB gains of the eight-channels of the eight RF/IF boards (Fig. 11). Across 4-8 GHz the LSB gains are in the range G_{LSB}=7-18 dB. Gains are greater towards the lower part of the band (around 2.5 GHz) and fall off at the highest frequencies (beyond ≈8.2 GHz). The measured LSB gains across the three narrow band filters (BPF-B, C and D) are shown in Fig. 12. All channels have very similar responses, with gains ≈10 dB.

Fig. 13 shows the measured results of the image sideband rejection versus LSB frequency across the ≈2-9 GHz band for the four band pass filters. The image sideband rejection with BPF-A (red curves) has minima IR≈20 dBc at the center of the IF band (≈510 MHz) and reaches values greater than ≈40 dBc towards the IF band edges (at 375 MHz and 650 MHz). Selecting the narrow band filters BPF-B, BPF-C and BPF-D allows operating the receiver with much improved rejection, of order ≈60 dBc, as a result of the combined effect of the mixer sideband separation and of the filter rejection.

We measured the noise figure (NF) of the WS RF/IF chains using the FSV Signal Analyser from Rohde and Schwarz coupled with a noise source (Noisecom NC3104, ENR≈15.6 dB at 5 GHz). The test results are shown in Fig. 14. The measurements refer to the board input SMA connector and include the signal chains up to the IF MCX connector. NF is in the range ≈8-16 dB across 4-8 GHz. For a given LO setting NF is minimum at the center of the IF band and increases towards the band edges. We note that NF value is lower for the wideband filter BPF-A than for the three narrow band filters BPF-B, C and D. This was expected from simulation as the insertion loss in front of the first amplifier on the WS board, which impacts the noise, is greater for the narrow-band filters.

Starting from the measured WS noise values, we evaluated the impact of the noise added to the entire PHAROS2 receiver chain. In particular, we estimated the noise temperature that would be obtained at the input of a cryogenically cooled PHAROS2 LNA (Low Noise Factory LNF-LNC4_8C) by cascading it to the WS (through coaxial cables assumed to have insertion loss of order ≈2 dB). The average noise temperature and gain performance of the cryogenic LNAs are T_N≈2.3 K and G≈39 dB, respectively. The predicted noise temperature of the receiver chain at the cryogenic LNA input, assuming there are no mutual effects and noise coupling between the antenna elements, is shown

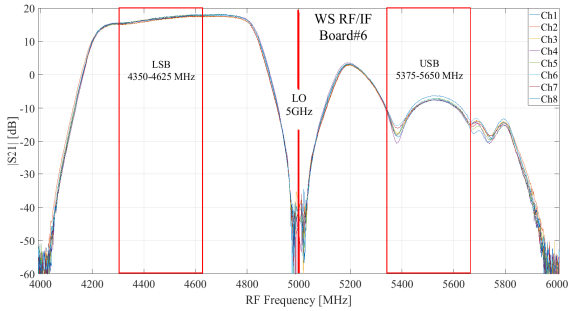

Fig. 10. VNA measured transmissions of the eight channels of one of the WS RF/IF boards by selecting filter BPF-A and LO frequency 5 GHz.

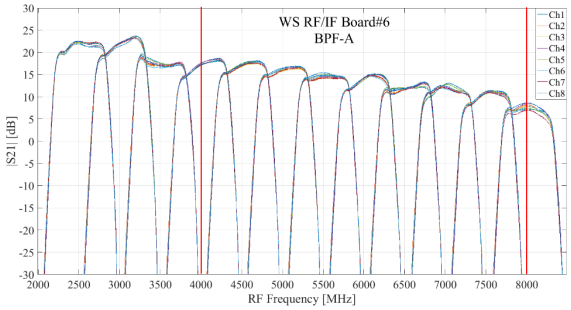

Fig. 11. Lower side band (LSB) gains of the eight channels of WS RF/IF Board #6 measured from the SMA RF input connector to MCX IF output connector with filter BPF-A. Cumulated measurements from 12 different LO frequency settings, ranging from 3 GHz to 8.5 GHz by 0.5 GHz steps. The power level was set at −5 dBm for the LO and −30 dBm for the RF.

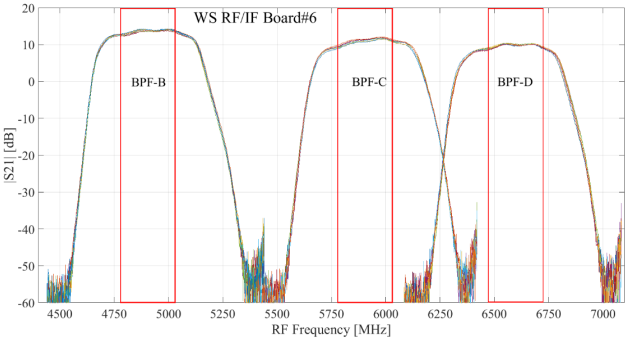

Fig. 12. Measured LSB gains of the eight channels of WS RF/IF Board #6 measured from the SMA RF input connector to MCX IF output connector for filters BPF-B, C and D.

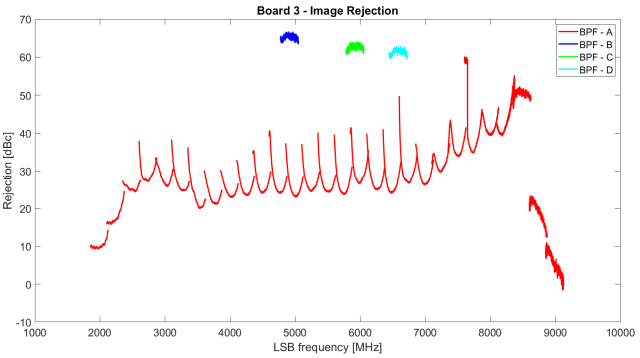

Fig. 13. Image sideband rejection measured for one of the channels (ch.1) of WS RF/IF Board #3 across the four different band pass filters. The ≈2-9 GHz LSB signal frequency for BPF-A was covered by 29 different LO frequency settings (red curves). Measured image rejection across BPF-B, C and D are shown by curves in dark blue, green and light blue, respectively. For each given LO frequency, the rejection values refer to the 375-650 MHz IF frequency band (275 MHz bandwidth).

978-1-7281-3049-1/19/$31.00 ©2019 IEEE

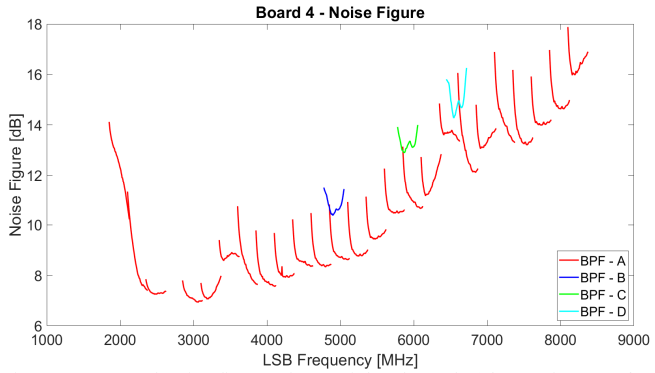

Fig. 14. Measured noise figure of one of the channels (ch. 1) of WS RF/IF Board #4 across the four different band pass filters. The bandwidth are 275 MHz wide for each of the different LO settings.

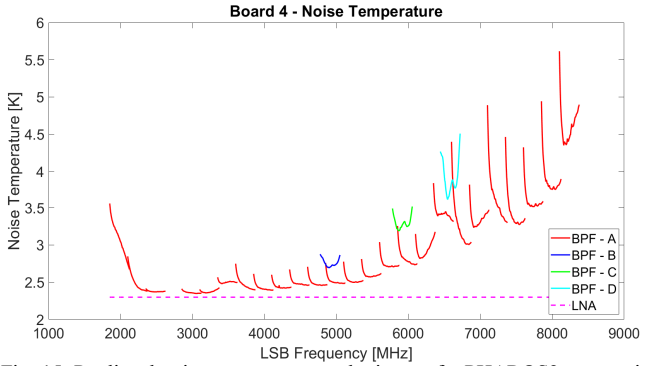

Fig. 15. Predicted noise temperature at the input of a PHAROS2 cryogenic LNA (T_N≈2.3 K, pink dashed line) cascaded to the warm receiver section.

in Fig. 15. Across the nominal RF range of PHAROS2, 4-8 GHz, the receiver noise temperature falls in the range 2.5-3.5 K for operation around the center of the IF band (at 512.5 MHz). A slight increase of noise, up to values of 5 K, is predicted for operation at the edges of the IF band. Although the cryogenic LNA operates across 4-8 GHz, in order to generate the plot of Fig. 15, we assumed the amplifier could perform with same in-band noise and gain (G≈39 dB) across the entire LSB frequency range ≈2-8.5 GHz. We point out that the measured Double Side Band (DSB) noise temperature T_{NDSB} is essentially equivalent to Single Side Band (SSB) noise temperature T_{NSSB}, as the sideband rejection is greater than 20 dBc: $T_{NSSB}=T_{NDSB}(1+G_{USB}/G_{LSB})\approx T_{NDSB}$.

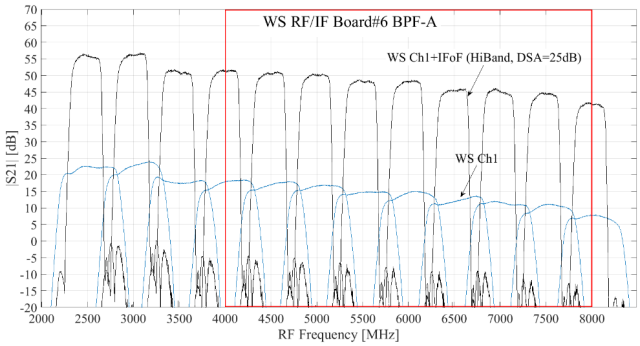

Fig. 16. Measured gain of Board #6 for 12 different LO frequency settings, from 3 GHz to 8.5 GHz by 0.5 GHz steps: including IFoF link with DSA = 25 dB (black curves) and without IFoF link (blue curves). The vertical red lines at 4 and 8 GHz delimit the nominal band edges of PHAROS2.

We tested the WS receiver with IFoF link. The average gain across 4-8 GHz is G_{LSB}≈50 dB when the digital step attenuator of the ORX is set to DSA=25 dB. The gain can be varied from ≈45 dB to ≈75 dB by changing the DSA from 31 dB to its 0 dB minimum attenuation. The measurement results are shown in Fig. 16.

IV iTPM DIGITAL BACKEND FOR PHAROS2

The iTPM is a FPGA-based processing module developed for SKA LFAA [10], [14] by an INAF-led collaboration with industrial partners. The PHAROS2 digital backend is based on the iTPM hardware, version 1.2. We modified the firmware to perform, on the iTPM, the digital beamforming synthesis of the signals from the PHAROS2 antenna elements.

PHAROS2 can simultaneously synthesize up to four beams, which can be integrated with a variable integration time (from 50 µsec to 1 sec) for on-the-fly (OTF) mapping as well as for discrete pointing observations (raster-scan mapping, pulsar search etc.). Furthermore, all of the four raw voltage data can be managed; however, such a configuration is used only for pulsar timing, for which a single beam is needed. Thus, only a single beam is retrieved, whereas the others are discarded. All the data are sent to the 40 GbE network and further processed by other computing nodes (CPU, GPU). A schematic diagram showing the implementation of the beamforming is shown in Fig. 17.

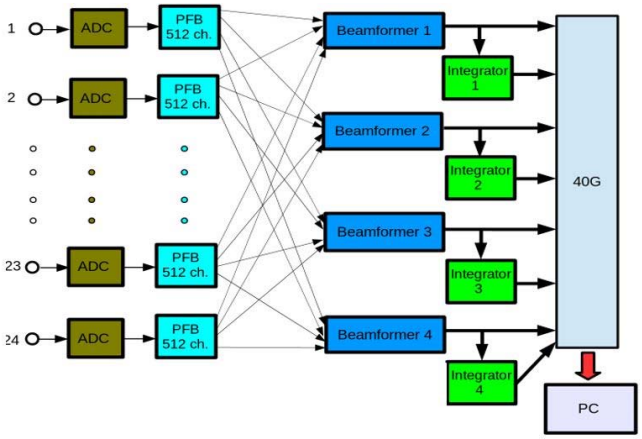

Fig. 17. Schematic diagram illustrating the implementation of the beamforming in the iTPM FPGAs for 24 single-polarization antenna elements. Four beams can be digitally synthesized, each provided with integrated spectra and with non-integrated spectra.

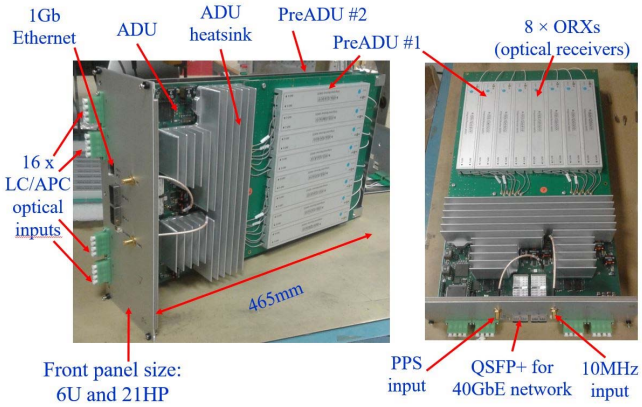

Fig. 18. iTPM digital backend consisting of the Analog Digital Unit (ADU) and of two preADU boards. Each preADU boards contains eight fiber-optics receivers (ORXs).

The iTPM consists of the Analog Digital Unit (ADU) and of two preADU boards (Fig. 18). The ADU is a 6U board containing sixteen dual-inputs Analog to Digital Converters (ADC) and two FPGAs (Xilinx Kintex Ultrascale XCU40) capable of digitizing and processing up to 32 RF input signals. Although the ADU was conceived mainly for the 50-350 MHz low frequency band, its use proved to be effective also for the 375-650 MHz high frequency band, therefore being suitable to process the IF signals from the PHAROS2 warm receiver section. The preADU board is based on eight ORXs each of which includes a band selector with a filter bank (low band 50-375 MHz used for LFAA, or high band 375-650MHz used for PHAROS2) and a switch to divert the IF input of any receiver on a 50 Ω load for debugging procedures.

The ADU is capable of acquiring and processing up to ≈500 MHz bandwidth radio-frequency streams from 32 single-polarization antennas (or 16 dual-polarization antennas). The ADU adopts 2 x 40Gbps Ethernet interfaces (QSFP), one for each FPGA, and high speed internal bus to connect the two FPGAs (25 Gbps + 25 Gbps bidirectional). Data processing includes channelization of the sampled data for each antenna based on an oversampling polyphase filterbank architecture (oversampling factor 32/27) with 512 spectral channels and beamforming on the FPGAs. The ADCs (AD9680, 1GS/s) are set to a sampling rate of 700 MS/s, thus the 375-650 MHz IF band (275 MHz bandwidth) is sampled in the second Nyquist window. The primary channels have a bandwidth of 810 kHz and are spaced of 684 kHz. We note that in PHAROS2 the signals are reversed twice in frequency: a first time in the WS, due to LSB tuning, and a second time in the digital backend, due to operation on the second Nyquist window. This double inversion results in non-reversed passbands.

Fig. 19 shows the digital backend cabinet hosting the iTPM and a computing server for post-processing and data storage. The power consumption of the iTPM is ≈150 W.

A. Power level consideration and DSA settings

The digital step attenuators of the preADUs can be remotely set by a software installed in the server. The value of the DSA determines the power level at the input of the ADCs. The signal sampled from the ADC must remain in a definite range, with a Root Mean Square (RMS) amplitude comprised from 15 to 30 ADC units, in order to guarantee proper operations [14]. Lower amplitude levels result in excess quantization noise, while higher amplitudes introduce nonlinearities due to clipping of the noise-like signal. Considering the possibilities of a sudden variation of the input signal during radio astronomy observations, due to RFI, it is advisable to keep the signal level in the range 15 to 20 ADC units and to set the DSA accordingly. This corresponds to setting a power level at the preADU output (ADU input) in the range from -3 dBm to 0 dBm.

The low-noise PHAROS2 front-end will be installed on a radio astronomy antenna that will look at sources towards the cold sky in C-band. The system noise temperature at the input of each of the cryogenic LNAs (cascaded to the Vivaldi antennas) is mainly dominated by the atmospheric

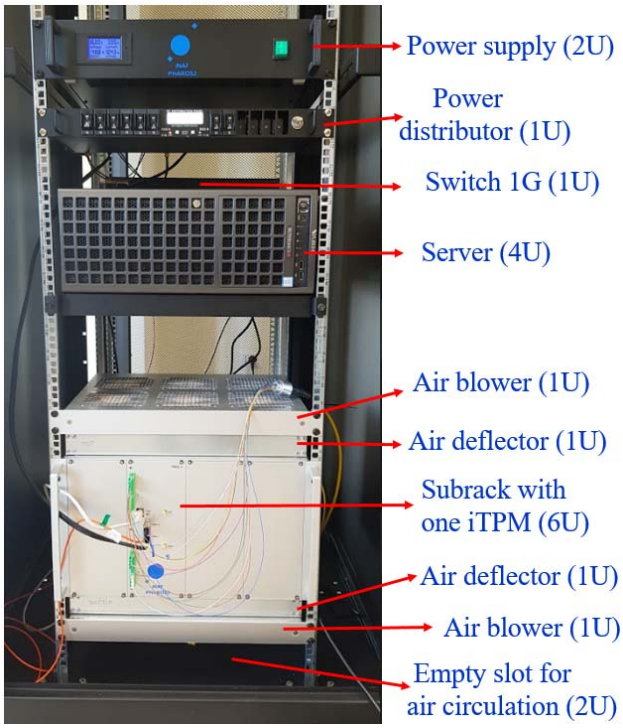

Fig. 19. Digital backend cabinet showing a subrack with one iTPM and air blower for air circulation (bottom), the server, the power supply, the power distributor and the network switch (top).

contribution (including spillover) and by the receiver noise. The atmospheric contribution is elevation-dependent and is minimum for antenna pointing at the Zenith. Therefore, the minimum system noise temperature is expected to be roughly of order 30 K, having assumed ≈20 K contribution from the atmosphere and ≈10 K contribution form the receiver (including optics losses, Vivaldi antenna losses, LNA noise, WS noise, etc.). Thus, the equivalent noise power spectral density at the cryogenic LNA input is of order -124 dBm/MHz. After amplification by the cryogenic LNA (G≈39 dB) the level on noise spectral density at the WS input will be of order -87 dBm/MHz (assuming ≈2 dB of insertion loss due to coaxial cables). The gain of the WS RF/IF module, from its SMA input connector to the MCX IF output connector (in front of the optical link) is of order G≈15 dB (Fig. 11). Thus, the power level at the input of the OTXs, integrated over the ≈300 MHz instantaneous IF bandwidth, is of order -47 dBm. To obtain the desired power level at the ADU input (≈-2 dBm), the required amplification by the IFoF link should be set to a gain G=45 dB, i.e. with DSA≈15 dB.

For noise testing purposes the PHAROS2 antenna would be pointed at a room temperature calibration load (≈293 K) rather than toward the cold sky. In this case the power level expected at the OTX inputs, integrated over the ≈300 MHz instantaneous IF bandwidth, will be of order -37 dBm. This requires setting the DSA at ≈25 dB. The power level settings indicated above allows to operate the link 20 dB below the input P1dB compression point of the IFoF link.

In the above consideration we assumed that no RFI is present across the observed band.

V Conclusion

We presented the development of a 32-channel room temperature heterodyne receiver and of a digital beamformer for the PHAROS2 (Phased Arrays for Reflector Observing Systems 2) Phased Array Feed (PAF). The room temperature receiver (WS) is the signal chain section located between the cryogenically cooled antenna array and the digital beamformer that will enable first-ever radio astronomy observation in C-band with a PAF.

The WS is based on four identical eight-channel radio frequency (RF)/intermediate frequency (IF) modules that in total are capable of analogue-processing 32 × RF signals across the 2.3–8.2 GHz frequency range. The heterodyne receivers are based on sideband separating schemes and downconvert the Lower Side Band (LSB) signals from each antenna to the 375-650 MHz IF frequency range (275 MHz bandwidth), which is suitable for further processing by the digital backend. The Upper Side Band (USB) is internally terminated on the PCB board (not extracted).

The first section of the WS RF/IF modules adopts a pre-filtering section based on a switchable filter bank to select one among four possible bandpass filters: a wideband BPF-A covering 2.3-8.2 GHz or one of three ≈300 MHz bandwidth BPF-B, C and D centered around astronomical lines. The filter bank section is cascaded with an RF amplification stage followed by the sideband separating mixer and by an IF filtering and IF amplification section. All the above functionalities of each WS RF/IF module are implemented on a four-layer PCB with surface-mounted components. The WS RF/IF module includes analogue fiber-optic transmitters (OTXs) for the IF signal transportation to the backend, where two IFs are sent over a single-mode optical fiber.

Across the nominal 4-8 GHz PHAROS2 RF band, by selecting BPF-A, the WS RF/IF chains deliver a gain in the range 7-18 dB (≈15 dB at 6 GHz) and a minimum image sideband rejection (ratio of gains in the LSB and the USB, G_{LSB}/G_{USB}) of ≈23 dBc for all channels, when referring to the MCX IF output connector of the PCB (IFoF optical links excluded). The measured gains and image sideband rejection, if selecting filters BPF-B, C or D, are ≈10 dB and ≈60 dBc, respectively. The gain of the IFoF link can be set in the range 29-60 dB by varying a digital step attenuator level in the range DSA=0-31 dB. Thus, the total gain of WS plus IFoF link can be adjusted to fall in the range ≈44-75 dB (at ≈6 GHz). The measured noise figure of the WS RF/IF receivers fall in the range ≈8-16 dB for all filters.

The digital backend is based on the iTPM (Italian Tile Processing Module), a processing module developed for the Square Kilometer Array Low Frequency Aperture Array. We described the development of the PHAROS2 digital beamformer, which can simultaneously synthesize one beam with non-integrated spectra and up to four beams with integrated spectra on the iTPM FPGAs (Field Programmable Gate Arrays). The beams are implemented for the 24 active single-polarization antenna elements of the PHAROS2 array across a 275 MHz instantaneous bandwidth.

References

[1] J.R. Fisher, R.F. Bradely, "Full-sampling array feeds for radio telescopes," Proceedings of SPIE Astronomical Telescopes and Instrumentation, Vol 4015, 2000.

[2] K. Warnick, R. Maaskant, M.V. Ivashina, D.B. Davidson, B.D. Jeffs, "High-Sensitivity Phased Array Receivers for Radio Astronomy, Proceedings of the IEEE, Vol. 104, Issue 3, pp. 607-622, March 2016.

[3] D. Anish Roshi et al., "Performance of a highly sensitive, 19-element, dual-polarization, cryogenic L-band phased array feed on the Green Bank Telescope," The Astronomical Journal, 155:202, May 2018.

[4] J. Simons, M. Ivashina, J. G. b. d. Vaate, and N. Roddis, "Beamformer system model of focal plane arrays in deep dish radio telescopes," European Radar Conf. EURAD 2005, Paris, France, 3-4 October 2005.

[5] J. Simons, J.G. Bij de Vaate, M.V. Ivashina, M. Zuliani, V. Natale, N. Roddis, "Design of a focal plane array system at cryogenic temperatures," Proc. 'EuCAP 2006', Nice, France, 6–10 Nov. 2006.

[6] W. Ciccognani, F. Di Paolo, F. Giannini, E. Limiti, P.E. Longhi, A. Serino, "A GaAs Front-end Receiver for Radio Astronomy Applications," 13th IEEE Melecon 2006, May 16-19, Spain.

[7] L. Liu, K. Grainge, and A. Navarrini, "Analysis of Vivaldi array antenna for phased array feeds application," IEEE MTT-S Int. Conf. on Num. Elec. and Multiph. Mod. and Opt. for RF, Micr., and THz App. (NEMO), Seville, Spain, 17-19 May, 2017.

[8] A. Navarrini, J. Monari, A. Scalambra, A. Melis, R. Concu, G. Naldi, A. Maccaferri, A. Cattani, P. Ortu, J. Roda, F. Perini, G. Comoretto, M. Morsiani, A. Ladu, S. Rusticelli, A. Mattana, P. Marongiu, A. Saba, M. Schiaffino, E. Carretti, F. Schillirò, E. Urru, G. Pupillo, M. Poloni, T. Pisanu, R. Nesti, G. Muntoni, K. Zarb Adami, A. Magro, R. Chiello, L. Liu, K. Grainge, M. Keith, M. Pantaleev, W. van Cappellen, "Design of PHAROS2 Phased Array Feed," Proc. of 2nd URSI Atl. Radio Sci. Meet. (AT-RASC), Gran Canaria, Spain, 28 May – 1 June 2018.

[9] A. van Ardenne, J.D. Bregman, W.A. van Cappellen, G.W. Kant, J.G. Bij de Vaate, "Extending the Field of View with Phased Array Techniques: Results of European SKA Research." Proc. IEEE 2009, 97, 1531–1542.

[10] G. Naldi, G. Comoretto, R. Chiello, S. Pastore, G. Pupillo, A. Mattana, A. Melis, R. Concu, M. Alderighi, A. Aminaei, J. Baker, C. Belli, S. Chiarucci, S. D'Angelo, G. Dalle Mura, A. De Marco, R. Halsall, A. Magro, J. Monari, A. Navarrini, F. Perini, M. Poloni, M. Roberts, S. Rusticelli, M. Schiaffino, F. Schillirò, E. Zaccaro, K. Zarb Adami, "Development of a new digital signal processing platform for the Square Kilometer Array." Proc. of 2nd URSI Atl. Radio Sci. Meet. (AT-RASC), Gran Canaria, Spain, 28 May – 1 June 2018.

[11] A. Navarrini, R. Nesti, L. Schirru "Electromagnetic simulation and beam-pattern optimization of a C-band Phased Array Feed for the Sardinia Radio Telescope." To be published in Proc. of IEEE UKRCON Conf, July 2-6, 2019.

[12] A. Navarrini, A. Scalambra, S. Rusticelli, A. Maccaferri, A. Cattani, F. Perini, P. Ortu, J. Roda, P. Marongiu, A. Saba, M. Poloni, A. Ladu, L. Schirru, "The Room Temperature Multi-Channel Heterodyne Receiver Section of the PHAROS2 Phased Array Feed" MDPI Electronics, Vol. 8, Issue 6, 666, June 2019.

[13] A. Navarrini, A. Scalambra, S. Rusticelli, A. Maccaferri, A. Cattani, F. Perini, P. Ortu, J. Roda, P. Marongiu, A. Saba, M. Poloni, A. Ladu, "A 2.3-8.2 GHz Room Temperature Multi-Channel Receiver for Phased Array Feed Application." To be published in Proc. of IEEE UKRCON Conf, July 2-6, 2019.

[14] G. Comoretto, et al. "The Signal Processing Firmware for the Low Frequency Aperture Array." Journal of Astronomical Instrumentation, Vol. 6, n. 1, 201, 2017.

978-1-7281-3049-1/19/$31.00 ©2019 IEEE